Hindawi
Advances in Materials Science and Engineering
Volume 2023, Article ID 8573440, 9 pages
https://doi.org/10.1155/2023/8573440

Research Article

Effect of ZrB_2 Particles on Machining Parameters of AA7475 Alloy-Based Composites by Optimization Technique

C. R. Mahesha,[1] R. Suprabha,[1] R. Suresh Kumar,[2] Chirumamill Mallika Chowdary,[3] Viyat Varun Upadhyay,[4] M. Soumya,[5] Essam A. Al-Ammar,[6] Sivasankar Palaniappan,[7] and Abdi Diriba[8]

[1]*Department of Industrial Engineering and Management, Dr. Ambedkar Institute of Technology, Bangalore, Karnataka 560056, India*
[2]*Department of Mechanical Engineering, Sri Eshwar College of Engineering, Coimbatore 641202, India*
[3]*Department of Civil Engineering, Koneru Lakshmaiah Education Foundation, Guntur, Andhra Pradesh 522302, India*
[4]*Department of Mechanical Engineering, GLA University, Mathura, UP 281406, India*
[5]*Department of Computer Science and Engineering, SR University, Warangal, Telangana 506001, India*
[6]*Department of Electrical Engineering, College of Engineering, King Saud University, Saudi Arabia*
[7]*Department of Environmental Engineering and Energy, Poznan University of Technology, Poznan, Poland*
[8]*Department of Mechanical Engineering, Mizan Tepi University, Tepi, Ethiopia*

Correspondence should be addressed to Abdi Diriba; abdi@mtu.edu.et

Received 10 September 2022; Revised 8 October 2022; Accepted 15 October 2022; Published 2 February 2023

Academic Editor: Pudhupalayam Muthukutti Gopal

ZrB_2 particle-reinforced AA7475 is a potential material for high-performance aeronautical engine blades because of its exceptional characteristics. The machinability of ZrB_2/AA7475 metal matrix composites (MMC) is still a challenge because of the influence of ZrB_2 particles. The impact of ZrB_2 particulates on the machined parameters of ZrB_2/aluminum matrix composites was explored experimentally in order to meet the needs of industry. Additionally, the best machining circumstances for this type of material matrix composites were studied in this research. A surface roughness (R_a) and metal removal rate (MRR) multiobjective optimization model was built, and a set of ideal parameter combinations was produced, with the surface roughness of ZrB_2/AA7475 material matrix composites being lower than that of the nonreinforced alloys at the same cutting speed.

1. Introduction

Aeronautics and other industries have greatly benefited from particle-reinforced metal matrix composites (PRMMC), a new family of materials with improved features such as a greater ratio of mass to strength, a greater elastic modulus, and better resistance to wear and tear [1–3]. There are two ways to make PRMMCs, ex situ and in situ. Ex situ processes use a subsequent technique, such as stir casting, to incorporate reinforcements into the matrix after they have been synthesized separately [4, 5]. Ex situ composites frequently exhibit particle segregation and poor interface adhesion [6]. However, in situ composites are made by directly synthesizing reinforcement phases inside the matrix, which improves adhesion at surfaces and hence increases mechanical characteristics [7, 8]. At the same time, the majority of studies concentrate on the in-situ particle-reinforced MMCs' material preparation method [9]. Engineers need to know how to machine these high-performance materials in order to use them in their designs. Strengthening particles in matrix are known to be extremely abrasive. Because of this, it is difficult to machine MMCs, and the most common difficulties are tool wear and low surface quality. Also, the physical qualities [10]. In commercial practice, silicon carbide-particle-strengthened MMCs are frequently utilized since the preparation method for ex situ material matrix composites is significantly less difficult [11, 12]. SiC particle-strengthened material matrix composites have been the

subject of much investigation on wear resistance, surface integrity, and the creation of chips [13].

Machining in situ MMCs, however, has received little attention. MMC grinding behaviour was investigated by [14, 15]. Surface quality was improved when removing PTMCs from titanium-6aluminium-4V by using a small depth of cut and a higher workpiece speed. The experimental results demonstrate that the brazed CBN wheel has a higher benefit in terms of higher polishing of PTMCs than the electroformed CBN wheel. MMCs with Al-6061-ZrB_2 were machined by [16, 17]. Cutting parameters were examined in relation to tool wear, force of cutting, and surface roughness. In terms of polishing PTMCs, it was observed that the brazed CBN wheel had an advantage over the electroformed CBN wheel [18, 19] for its machinability. The effect of factors on performance metrics and the built-up edge and chip creation are studied during turning operations. Using Al_2O_3 and Al_2O_3-SiC as a baseline [20, 21], evaluated the machinability of their innovative in situ ceramic strengthened aluminium MMC. An analysis by [22] examined the mechanical behavior of ZrB_2/Al7475MMC. Chip formation, tool wear, and surface quality are all discussed. Findings from a study showed that PCD tools were less prone to tool wear than PCBN and layered carbide tools. The most typical reasons for tool failure include wear from abrasion, adhesion, chipping, and peeling. Unlayered carbide tools have a tool life ranging from three to twenty minutes, with milling speed having the greatest impact [23, 24].

Cutting circumstances for MMCs are the most important part of a machining operation. When LM23 Al/SiC particle composites were turned by [25, 26], it was discovered that the surface finish was impacted by machining parameters. The best conditions for increasing metal removal rate while reducing surface roughness were found utilizing RSM. A want function technique was utilized by [27] to optimize machining parameters in order to decrease surface roughness. V, f, and a_p all affect flank wear and R_a in spinning aluminum/silicon carbide particle MMC with an unlayered WC addition in a dry environment [28]. A Taguchi approach was utilized to discover the optimum mixture of flank wear and R_a characteristics [29]. Soft computing has also been used by certain researchers to help them better optimize cutting parameters. The surface roughness of aluminum-silicon carbide (20p) was investigated by [30, 31] utilizing PCD additions under various cutting circumstances. ANOVA and ANN approaches were used to analyze the experimental data. Al/SiC MMCs were turned utilizing a PCD insert in an experiment conducted by [32] a link was found among speed of cutting, feed and cut depth as well as workpiece's surface finish and particular power [33]. GRA was utilized to determine the best machining constraints. For aluminum/SiCp MMCs being turned in a dry environment with an unlayered WC addition to cutting speed, feed rate, and cut depth have an effect on flank wear and surface roughness. The ideal combination of wear of flank and surface roughness properties was discovered utilizing the Taguchi technique. On the basis of these findings [34, 35], we studied the outcome of cutting speed, feed rate, depth of cut, and cutting force on Al6061-TiC surface roughness utilizing a Taguchi L27 orthogonal array and ANOVA. Numerous studies on the mechanical parameters and cutting characteristics of material matrix composites supplemented with ex situ particles have been conducted. Ex situ MMCs have different mechanical properties than in situ MMCs because of their distinct microstructures [36–38]. Due to these differences in machinability, only a small amount of research has been done on the machining parameters and cutting parameters for in situ material matrix composites. Additionally, for industrial purposes, machining efficiency is a significant metric. A ZrB_2-reinforced MMCs sample is machined with various cutting parameters to research the impact of reinforcement particles on machining force and surface roughness. We also developed, based on our experimental findings, an approach to finding the best machining parameter combinations that takes both MMR and surface roughness into consideration. To summarize the paper's organization, consider the following: Section 2 goes into great depth on the machining test circumstances. Section 3 presents and discusses the experimental outcomes. GA is used in Section 4 to establish and develop the multi-objective optimization model. Here are the final thoughts and plans for further research in Section 5.

2. Experimentation

2.1. Materials. Alloys of 7475 aluminium and ZrB_2 (ZrB_2 particles range in size from 50 nm to 200 nm) were employed in this experiment, and the mixed salts method was used to make the ZrB_2 particles. Table 1 shows the theoretical chemical composition (weight percentage) of a matrix alloy. It is tabulated in Table 2 that ZrB_2/AA7475 MMCs in situ have the following mechanical and physical properties. They were fashioned from square blocks of ZrB_2/AA7475 MMCs using the turning method, respectively.

2.2. Turning Criteria Used. A dry bar-turning approach was used on a computer numerical control turning center for the experiments. PCD tools were used in this experiment because the ZrB_2 particles were so aggressive in their ability to scratch and abrade surfaces. Table 3 contains the relevant turning conditions.

2.3. Evaluation. Figure 1 depicts the cut-off force metering apparatus. All forces are radial forces: Fc (cutting) and Ft (pushing). A surface roughness tester (T620A) was utilized to evaluate the roughness of the surface with a calculation and cut-off length of 0.8 mm. The average values of the measurements made at each position were calculated after they were repeated twice.

3. Analysis of Experimental Result

3.1. Machining Forces. For a variety of cutting speeds, feed rates, and cutting forces, the results are shown in Figures 2 and 3. In comparison to ZrB_2/Al MMCs, the nonreinforced 7475 aluminium alloy has a lower cutting force. The cutting and thrust forces for 7475 aluminium alloy and MMCs are

Table 1: Chemical arrangement of AA 7475 alloy.

Basics	Copper	Chromium	Magnesium	Zinc	Manganese	Silicon	Aluminium
wt%	1.9	0.22	2.3	5.7	0.06	1.50	Remaining

Table 2: ZrB_2/AA 7475 MMCs mechanical and physical characteristics.

Properties	Elastic modulus (GPa)	Yield strength (MPa)	Density (g/cc)	Elongation	Hardness (HB)	Poisson ratio
Range	71.7	462	2.81	12%	140	0.33

Table 3: Turning criteria.

Turning criteria	Description
Cutting speed (V) (m/min)	30, 60, 90, 120
Feed rate (f) (m/min)	30, 60, 90, 120
Depth of cut (a_p) (mm)	0.5, 1, 1.5, 2
Cutting edge angle (°)	−5
Cutting condition	Dry
Cutting tool	Polycrystalline diamond
Nose radius (mm)	0.6
Clearance angle (°)	5

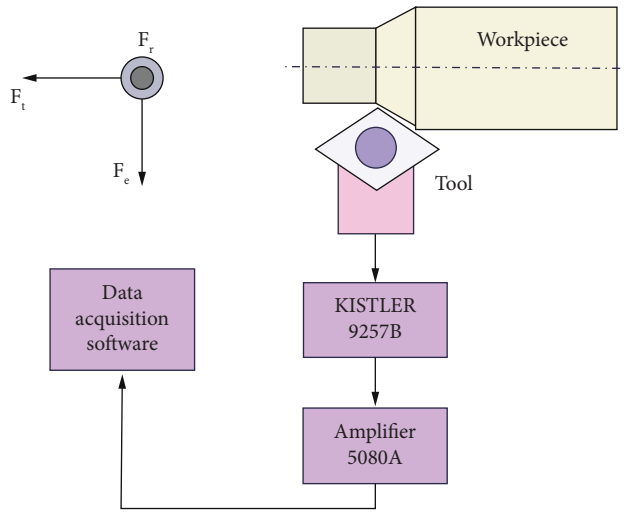

Figure 1: Illustration of cutting force arrangement.

illustrated in Figures 2(a) and 2(b). Cutting speed has an important impact on both cutting and pushing forces. While MMCs are travelling at speeds of less than 60 m/min, the forces diminish rapidly as speed rises.

The force rises significantly as speed is increased further. The following is a summary of how this works:

(1) When cutting speed increases, the tool-to-workpiece friction ratio decreases.

(2) As cutting speed increases, the cutting temperature rises, softening the metal matrix. Because of the two factors outlined above, as the speed of cutting grows from 10 m/min to 60 m/min, the force becomes less significant.

Cutting and pushing forces are depicted in Figure 3 using various feeds. MMCs have a greater tensile strength than the aluminium alloy 7475. As feed increases, so do the pressures for both resources practically linearly. As feed rate rises, the MRR rises, which necessitates a greater amount of energy for chip creation. The cutting force is increased as a result. In contrast, MMCs have a far greater growth rate than the 7475 aluminium alloy. The forces exerted by the two materials are nearly equal at low feed rates. Because of the presence of reinforced particles in ZrB_2/Al 7475 MMCs, the shear stress rises with increasing feed rate. As inputs rise, the differential between MMCs and nonreinforced alloys widen. A nonreinforced alloy's thrust force is virtually unaffected by the feed.

To further our understanding of how reinforcements affect force generation, we analyzed the force signals from the dynamometer. Figure 4 depicts the highest forces generated while spinning MMCs and AA7475 at 90 m/min, 60 mm/min feed, and a 2 mm depth of cut at these various speeds. When MMCs are turned, the force of cutting is greater than radiated force. In contrast, when spinning AA7475, the highest force of cutting is less than the radiated force. This may have been caused by turning AA7475. AA7475 is less rigid than ZrB_2/AA7475 MMCs, which makes the workpiece more prone to vibration during the machining procedure. As an outcome, the cutting force will be greater than the maximum radial force. The V is greater than average radiated force while turning 7475 alloy. Cutting force during the turning of MMCs differs significantly from thrust force compared to AA7475, suggesting that ZrB_2/AA7475 MMCs are more heterogeneous due to the reinforcements. When turning both materials, the radiated force variation is greater than the force of the cutting and thrust force variations. This could be because of vibrations that occur throughout the turning operation.

3.2. Surface Roughness (R_a). Figure 5 illustrates how cutting speed influences surface roughness. ZrB_2/Aluminum material matrix composites have a lower roughness than nonreinforced 7475 aluminium alloy at all cutting speeds. Because of the reinforcing particles, ZrB_2/Al7475 MMCs are less ductile and more prone to fracture when turned. On the other hand, as seen in Figure 5, raising the cutting speed leads to lessened surface roughness. When cutting at a faster speed, there may be a decrease in material flow on the side. Figure 6 illustrates the surface roughness is influenced by feed rate. Maintaining a constant feed rate results in a linear increase in surface roughness. While the roughness of MMC is lower when fed at low speeds, the opposite is true when fed at high speeds.

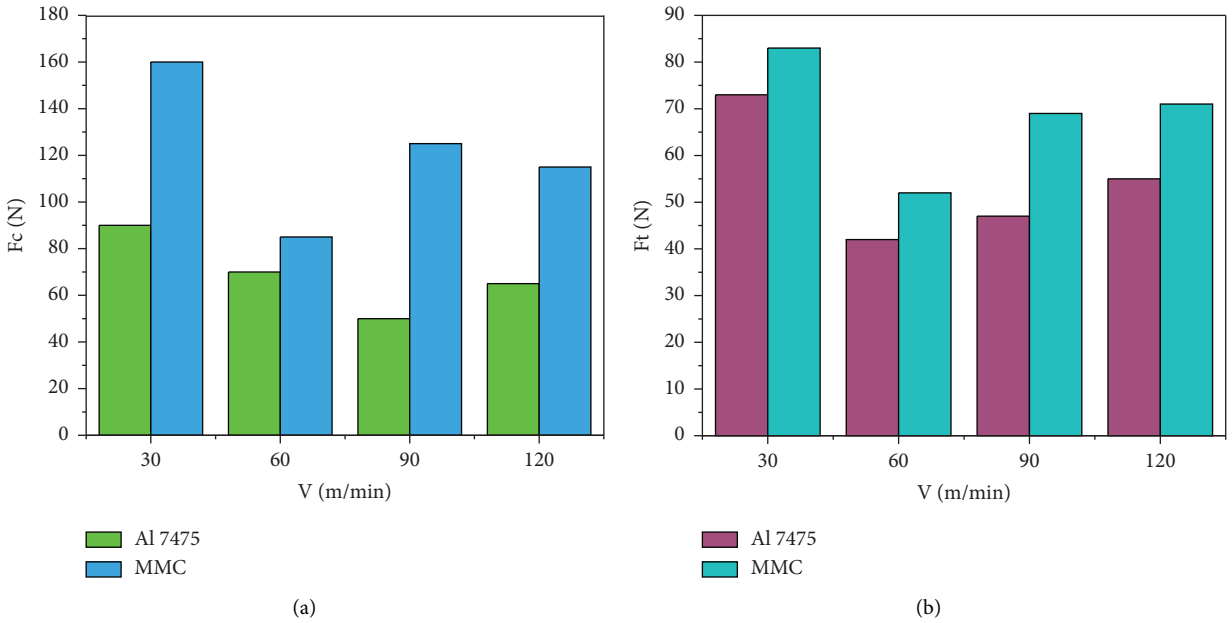

Figure 2: Comparison of (a) cutting force and (b) thrust force with speed (at $f = 60$ mm/min and $a_p = 2$ mm).

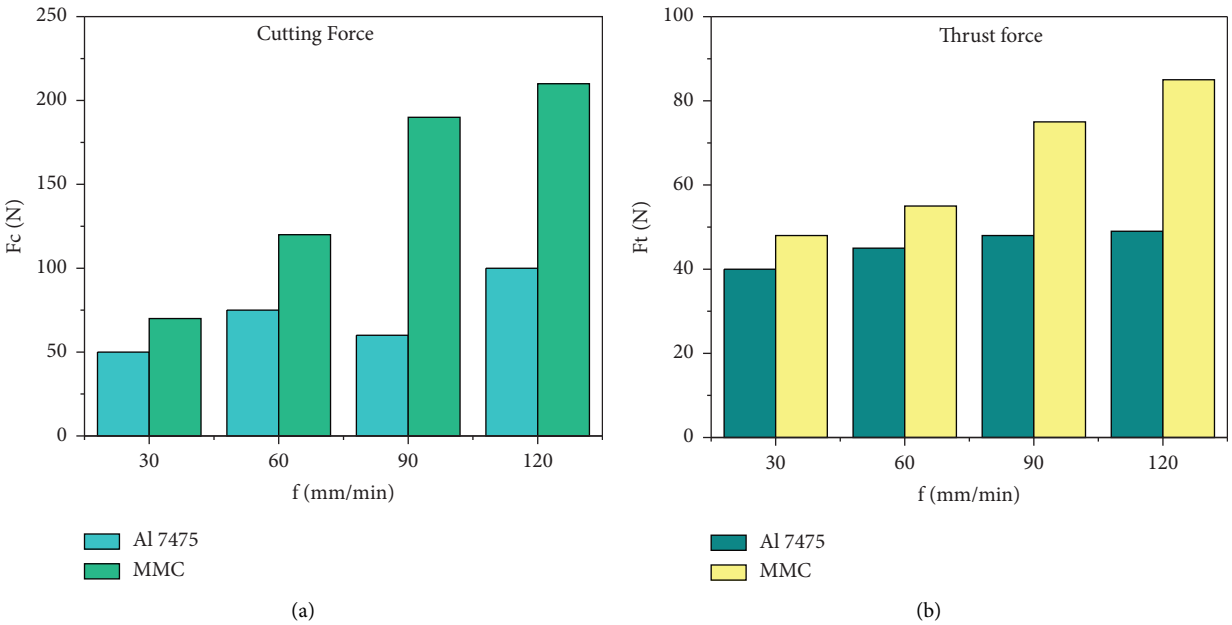

Figure 3: Comparison of forces with feed rate (at $V = 90$ m/min and $a_p = 2$ mm).

Feed marks on nonreinforced 7475 aluminium alloy are inconsistent because the material softens during cutting. When it comes to MMC, the feed markings are plainly visible, and the f marks become more severe as V increases. Reinforcement particles may be too little to have an effect on this. Because the ZrB_2 particle is so small, it has a small effect on the machining process.

4. Surface Roughness and Metal Removal Rate Improved by Optimizing Turning Parameters

Surface roughness is a more critical factor in determining the quality of a workpiece's surface, since abnormalities in the surface can serve as the nucleation point for fractures or corrosion. This section examined experimentally the

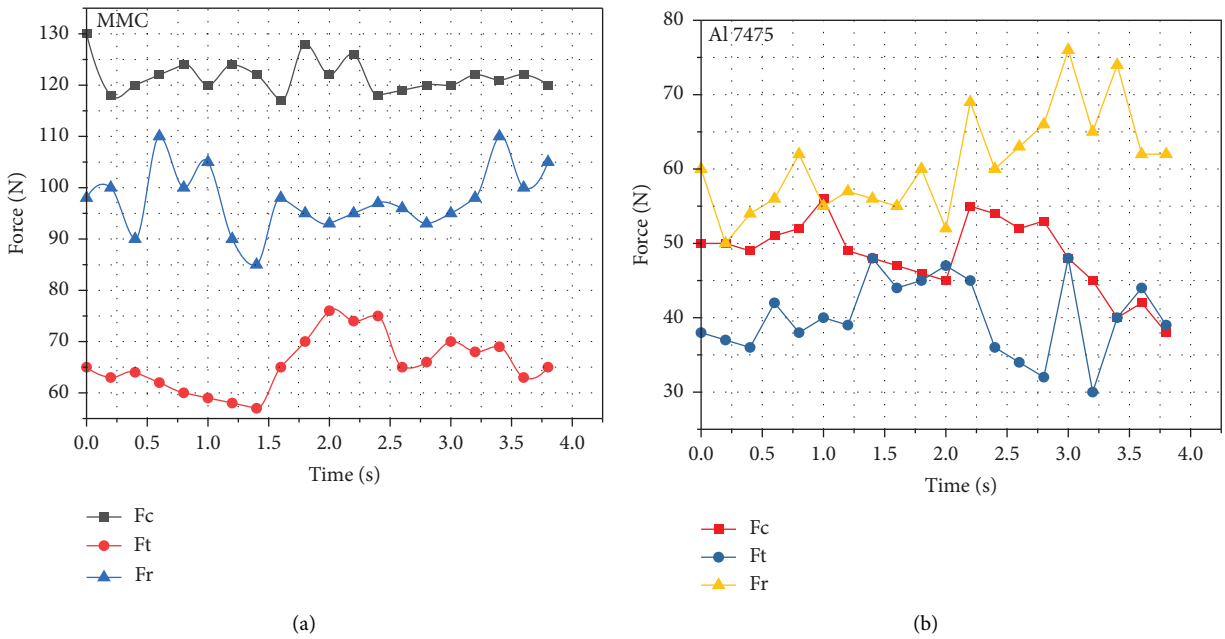

Figure 4: Comparison of force signals. (a) MMCs. (b) 7475 ($V = 90$ m/min, $f = 60$ mm/min, $a_p = 2$ mm).

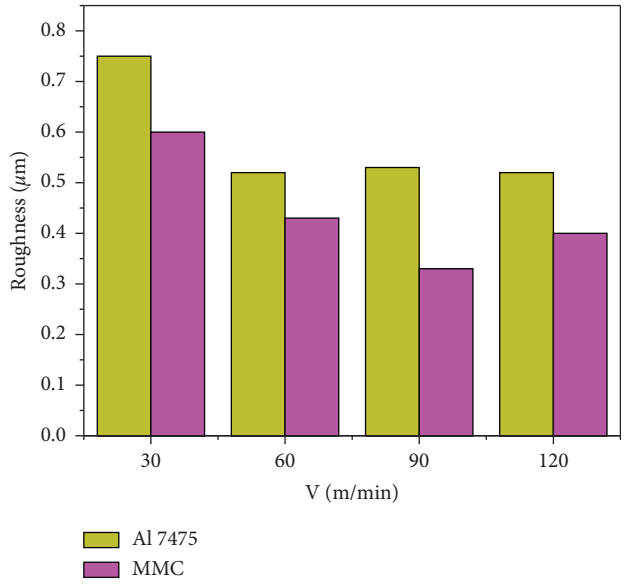

Figure 5: Comparison of V on R_a ($f = 60$ mm/min, $a_p = 2$ mm).

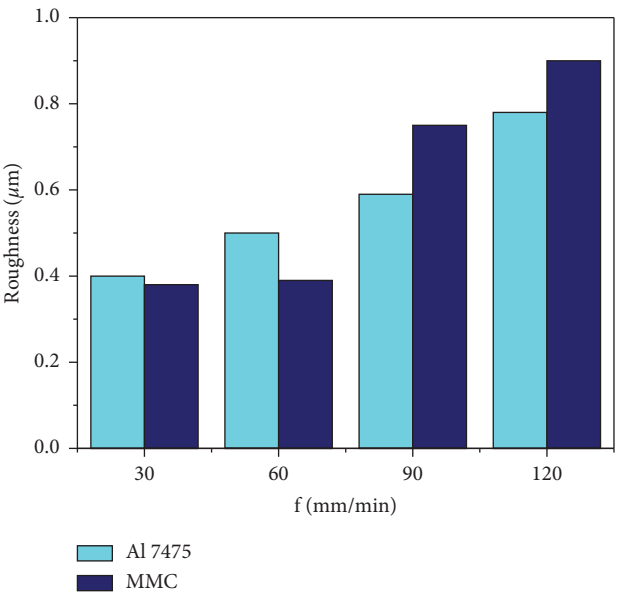

Figure 6: Impact of f (mm/min) on R_a ($V = 90$ m/min, $a_p = 2$ mm).

connection between V and R_a. The surface roughness model was built with RSM 32 to allow for quantitative comparisons between cutting settings and surface roughness. Real-world data can be depicted as a two- or three-dimensional hypersurface, utilizing RSM as a major tool for discovering and visualizing the relationship between variables. Surface roughness and MRR were also taken into consideration when optimizing the cutting parameters.

4.1. Development of the Surface Roughness Model. There are fewer design points in a Box–Behnken design than in central composite designs, making it more efficient at estimating first- or second-order coefficients. There are usually three layers of each element in a Box–Behnken design. The speed of the cutting range starts at 110 to 300 m/min, feed rates range from 30 to 120 mm/min, and the depth of cut ranges from 0.5 to 1.5 mm, making this machine versatile enough to handle a varied range of resources and applications. Table 4 shows the link among surface roughness and machine properties as follows:

According to earlier studies, a second-sort quadratics model can be used to approximate the true functional connection between R_a and cutting properties, which can be represented as

Table 4: Experimentation outcome on R_a.

S. no.	Cutting factor			Surface roughness (μm)
	V (m/min)	F (mm/min)	a_p (mm)	
1	30	120	0.5	3.12
2	60	90	0.5	4.64
3	90	120	1.5	2.21
4	120	120	1	1.72
5	120	90	1	1.63
6	90	30	1	0.31
7	60	90	1	1.84
8	30	60	1.5	0.86
9	60	120	1	8.24
10	90	30	1	0.62
11	120	60	1	1.74
12	120	90	1	0.63
13	90	120	0.5	0.63
14	30	30	0.5	0.53
15	60	60	1	1.75
16	120	90	1.5	3.53
17	90	120	1	1.72

Table 5: The model's statistical summary.

Basis	S.D.	R^2	Adj. R^2	Pred. R^2	Press
2FI	0.136496	0.9617	0.9526	0.9474	1.18614
Linear	0.160973	0.9458	0.9492	0.9304	1.59635
Quadratic	0.097193	0.9945	0.9872	0.9863	0.45731

$$R_{\mathrm{a}} = \beta + \sum_{i=1}^{k} \beta_i x_i + \sum_{i=1}^{k} \beta_{ii} x_i^2 + \sum \sum_{i<j} \beta_{ij} x_i x_j + \varepsilon, \quad (1)$$

where R_{a} is surface roughness of workpiece, β is regression coefficients, x_i is values of i^{th} cutting parameter, and ε is observation's mistake due to the experiment.

ANOVA was used to examine the effect of input variables on surface roughness in order to confirm the findings of past experiments. Models were compared using the linear, 2FI, and quadratic models to determine which one was the most accurate. Table 5 demonstrates that the quadratic model is a great fit, and hence the surface response function should be a quadratic model. Second order is the response surface model (RSM) data. The regression equation for R_a is shown as

$$R_{\mathrm{a}} = -2.33 - 0.0044V + 0.091f + 1.26a_{\mathrm{p}} - 0.00038\mathrm{Vf} + 0.0026Va_{\mathrm{p}} + 0.00062fa_{\mathrm{p}} + 0.000048V^2 + 0.00016f^2 - 1.11a_{\mathrm{p}}^2. \quad (2)$$

The original data used to create the regression model were utilized to verify the model's accuracy. In addition, three roughness values of the surface were utilized to verify the accuracy of RSM. Table 6 displays the results of the testing. There was good distribution in the space of cutting parameter selection for the checking data. As a result, the RS model's accuracy may be tested using these data. Table 6 shows that the maximum inaccuracy is less than 10%. As a result, the regression model has been proven to be accurate.

4.2. Optimum Results and Discussion. Both objectives of this research are at odds with one another. For example, the MRR increases as the feed rate rises, yet surface roughness also rises as the feed rate rises. The other goal (raising the MRR) would never be achieved if all efforts were directed just at smoothing the surface texture. With so many competing goals, it is essential to find a middle ground. Problems with several objectives are frequently tackled using the sum of weighted elements approach. There is typically just one answer per run, and the weights are normalized so that the sum of the weights equals 1. Initializing, evaluating, crossover and mutation, selection, and other GA processes are just a few of the many facets that go into the algorithm's construction. In order to optimize the multiobjective optimization model, commercial software was used. A relative experiment was conducted in order to confirm the best outcomes. It was necessary to use both optimal cutting parameters and conventional cutting parameters to achieve the appropriate surface roughness while cutting ZrB_2/AA7475. Table 7 shows the outcomes. Surface roughness has

Table 6: RS model's accuracy was tested using this collection of data.

Trial	Cutting factor			R_a		
	V	F	a_p	Measurement	*Rs* model	Error (%)
1	60	90	0.6	1.193	1.36212	7.909
2	90	120	0.8	1.805	1.97563	9.969
3	120	60	1.2	0.478	0.46119	6.415

Table 7: Comparison of experimental results.

Cutting type	Cutting factor			Surface roughness (μm)	MRR (mm^3/min)
	V (m/min)	F (mm/min)	a_p (mm)		
Conventional	120	120	1	1.72	14090000
Optimal	90	90	1	0.765	12143000

been demonstrated to improve with increasing cutting speed. When cutting at a faster speed, there may be a decrease in material flow on the side. As the feed rate rises, the roughness of the finished product also rises.

5. Conclusions and Scope of Future Work

The machining parameters of 6% ZrB_2/AA7475 material matrix composites must be studied for engineering applications because it is a new material. The nonreinforced 7475 aluminium alloy was utilized as a comparison to find the effect of in situ produced ZrB_2elements on the machining parameters of material matrix composites. Surface roughness and machining force were examined in relation to ZrB_2 particles. A surface roughness response surface model was created. The following are the study's most important findings:

(1) ZrB_2/AA7475 MMCs have a somewhat higher machining force than 7475 aluminium alloy without reinforcement. As the speed increased, so did the cutting and pushing forces for both substances. The machining force rose gradually after a specific speed of 60 m/min. The machining force rose in direct proportion to the feed rate. The forces generated by the two materials are almost equal when the feed rates are relatively low. Although the nonreinforced alloy has a higher initial machining force than ZrB_2/aluminum matrix materials, this increase is slower.

(2) Both materials saw significant reductions in surface roughness as the cutting speed was increased. Fewer cuts are made after a specific speed is reached. When fed at a low rate, ZrB_2/AA7475 MMCs have a rougher surface than 7475 aluminium alloy, but as the feed rate is increased, ZrB_2/AA7475 MMCs' surface roughness increases faster. On the other hand, the feed marks on ZrB_2/Al7475 MMCs are clearly visible. For this novel material, there is still much work to be done before a complete understanding of machinability can be acquired. In the near future, we plan to investigate the mechanisms that cause material loss and chip creation.

Data Availability

The data used to support the findings of this study are included within the article. Further data or information is available from the corresponding author upon request.

Conflicts of Interest

The authors declare that there are no conflicts of interest.

Acknowledgments

The authors appreciate the supports from Mizan Tepi University, Ethiopia for the research and preparation of the manuscript. The authors would like to acknowledge the Researchers Supporting Project Number (RSP2023R492), King Saud University, Riyadh, Saudi Arabia.

References

[1] S. R. Ruban, K. L. Dev Wins, J. D. Raja Selvam, and R. S Rai, "Influence of turning parameters on the machinability of Al6061/ZrB2 & ZrC hybrid in-situ Aluminium Matrix Composite," *Australian Journal of Mechanical Engineering*, vol. 2021, 2021.

[2] M. M. Nasr, S. Anwar, A. M. Al-Samhan, M. Ghaleb, and A. Dabwan, "Milling of graphene reinforced ti6al4v nanocomposites: an artificial intelligence based industry 4.0 approach," *Materials*, vol. 13, no. 24, pp. 1–22, 2020.

[3] D. Srinivasan, M. Meignanamoorthy, A. Gacem et al., "Tribological behavior of Al/Nanomagnesium/Aluminum nitride composite synthesized through liquid metallurgy technique," *Journal of Nanomaterials*, vol. 2022, pp. 1–12, Article ID 7840939, 2022.

[4] Z. Liao, A. Abdelhafeez, H. Li, Y. Yang, O. G. Diaz, and D. Axinte, "State-of-the-art of surface integrity in machining of metal matrix composites," *International Journal of Machine Tools and Manufacture*, vol. 143, pp. 63–91, 2019.

[5] V. Mohanavel, K. Ashraff Ali, S. Prasath, T. Sathish, and M. Ravichandran, "Microstructural and tribological characteristics of AA6351/Si3N4 composites manufactured by stir casting," *Journal of Materials Research and Technology*, vol. 9, no. 6, pp. 14662–14672, 2020.

[6] A. Pugazhenthi, I. Dinaharan, G. Kanagaraj, and J. D. R. Selvam, "Predicting the effect of machining parameters on turning characteristics of AA7075/TiB2 in situ

aluminum matrix composites using empirical relationships," *Journal of the Brazilian Society of Mechanical Sciences and Engineering*, vol. 40, no. 12, p. 555, 2018.

[7] T. Chwalczuk, D. Przestacki, P. Szablewski, and A. Felusiak, "Microstructure characterisation of Inconel 718 after laser assisted turning," *MATEC Web of Conferences*, vol. 188, p. 02004, 2018.

[8] R. Singh, M. Shadab, and R. N. Rai, "Optimization of machining process parameters in conventional turning operation of Al5083/B4C composite under dry condition," *Materials Today Proceedings*, vol. 5, no. 9, pp. 19000–19010, 2018.

[9] A. Pugazhenthi, G. Kanagaraj, I. Dinaharan, and J. David Raja Selvam, "Turning characteristics of in situ formed TiB2 ceramic particulate reinforced AA7075 aluminum matrix composites using polycrystalline diamond cutting tool," *Measurement*, vol. 121, pp. 39–46, 2018.

[10] C. Yan, W. Lifeng, and R. Jianyue, "Multi-functional SiC/Al composites for aerospace applications," *Chinese Journal of Aeronautics*, vol. 21, no. 6, pp. 578–584, 2008.

[11] S. Natarajan, R. Narayanasamy, S. P. Kumaresh Babu, G. Dinesh, B. Anil Kumar, and K. Sivaprasad, "Sliding wear behaviour of Al 6063/TiB2 in situ composites at elevated temperatures," *Materials & Design*, vol. 30, no. 7, pp. 2521–2531, 2009.

[12] L. M. Tham, M. Gupta, and L. Cheng, "Effect of limited matrix-reinforcement interfacial reaction on enhancing the mechanical properties of aluminium-silicon carbide composites," *Acta Materialia*, vol. 49, no. 16, pp. 3243–3253, 2001.

[13] I. Aziz, Z. Qi, and X. Min, "Corrosion inhibition of SiCp/5A06 aluminum metal matrix composite by cerium conversion treatment," *Chinese Journal of Aeronautics*, vol. 22, no. 6, pp. 670–676, 2009.

[14] C.-G. Zhou, L.-D. Wang, J.-W. Shen, C.-H. Chen, Y. Ou, and H.-T. Feng, "Wear characterization of raceway surface profiles of ball screws," *Journal of Tribology*, vol. 14411 pages, 2022.

[15] X. Liu, L. Cai, and H. Chen, "Residual stress indentation model based on material equivalence," *Chinese Journal of Aeronautics*, vol. 35, no. 8, pp. 304–313, 2022.

[16] X. F Liu, W. H Wang, R. S Jiang, Y. F Xiong, and C. W. Shan, "Comparative investigation on surface integrity for conventional and ultrasonic vibration–assisted cutting of in situ TiB2/7050Al MMCs," *International Journal of Advanced Manufacturing Technology*, vol. 120, no. 3–4, pp. 1949–1965, 2022.

[17] P. Maurya, N. Kota, J. Gibmeier, A. Wanner, and S. Roy, "Review on study of internal load transfer in metal matrix composites using diffraction techniques," *Materials Science and Engineering A*, vol. 840, p. 142973, 2022.

[18] L. Lü, M. O. Lai, Y. Su, H. L. Teo, and C. F. Feng, "In situ TiB2 reinforced Al alloy composites," *Scripta Materialia*, vol. 45, no. 9, pp. 1017–1023, 2001.

[19] X. Pan, W. He, Z. Cai et al., "Investigations on femtosecond laser-induced surface modification and periodic micropatterning with anti-friction properties on Ti6Al4V titanium alloy," *Chinese Journal of Aeronautics*, vol. 35, no. 4, pp. 521–537, 2022.

[20] F. Zhao, B. Lin, Y. He, and T. Sui, "Interference mechanism and damage accumulation in high-speed cross scratches on hard brittle materials," *Chinese Journal of Aeronautics*, vol. 35, no. 3, pp. 579–591, 2022.

[21] Ü. A. Usca, M. Uzun, S. Sap et al., "Tool wear, surface roughness, cutting temperature and chips morphology evaluation of Al/TiN coated carbide cutting tools in milling of Cu–B–CrC based ceramic matrix composites," *Journal of Materials Research and Technology*, vol. 16, pp. 1243–1259, 2022.

[22] X. Han, Z. Liao, G. G. Luna, H. N. Li, and D. Axinte, "Towards the understanding the effect of surface integrity on the fatigue performance of silicon carbide particle reinforced aluminium matrix composites," *Journal of Manufacturing Processes*, vol. 73, pp. 518–530, 2022.

[23] T. Tayeh, J. Douin, S. Jouannigot et al., "Hardness and Young's modulus behavior of Al composites reinforced by nanometric TiB2 elaborated by mechanosynthesis," *Materials Science and Engineering A*, vol. 591, pp. 1–8, 2014.

[24] M. Wang, D. Chen, Z. Chen et al., "Mechanical properties of in-situ TiB2/A356 composites," *Materials Science and Engineering A*, vol. 590, pp. 246–254, 2014.

[25] R. Aghababaei, M. Malekan, and M. Budzik, "Cutting depth dictates the transition from continuous to segmented chip formation," *Physical Review Letters*, vol. 127, pp. 235502–235523, 2021.

[26] S. Kesarwani and R. K. Verma, "Ant Lion Optimizer (ALO) algorithm for machinability assessment during Milling of polymer composites modified by zero-dimensional carbon nano onions (0D-CNOs)," *Measurement*, vol. 187, p. 110282, 2022.

[27] A. Dttmann and J. d. O. Gomes, "Evaluation of additive manufacturing parts machinability using automated gmaw er70s-6 with nodular cast iron," *U.Porto Journal of Engineering*, vol. 7, no. 2, pp. 88–97, 2021.

[28] M. El-Gallab and M. Sklad, "Machining of Al/SiC particulate metal-matrix composites Part I: tool performance," *Journal of Materials Processing Technology*, vol. 83, no. 1–3, pp. 151–158, 1998.

[29] X. Ding, W. Y. H. Liew, and X. D. Liu, "Evaluation of machining performance of MMC with PCBN and PCD tools," *Wear*, vol. 259, no. 7–12, pp. 1225–1234, 2005.

[30] N. H. Ononiwu, C. G. Ozoegwu, N. Madushele, and E. T. Akinlabi, "Characterization, machinability studies, and multi-response optimization of AA 6082 hybrid metal matrix composite," *International Journal of Advanced Manufacturing Technology*, vol. 116, no. 5–6, pp. 1555–1573, 2021.

[31] N. H. Ononiwu, C. G. Ozoegwu, N. Madushele, and E. T. Akinlabi, "Machinability studies and optimization of aa 6082/fly ash/carbonized eggshell matrix composite," *Revue des Composites et des Matériaux Avancés*, vol. 31, no. 4, pp. 207–216, 2021.

[32] S. Mohanty, G. K. Mohanta, S. R. Das, and J. J. Behera, "The effect of process parameters while turning AL based MMC with waste reinforcement in CNC machine in wet condition by using Taguchi optimization technique," *MATERIALS, MECHANICS & MODELING (NCMMM-2020)*, vol. 2341, 2021.

[33] R. K. Bhushan, S. Kumar, and S. Das, "Effect of machining parameters on surface roughness and tool wear for 7075 Al alloy SiC composite," *International Journal of Advanced Manufacturing Technology*, vol. 50, no. 5–8, pp. 459–469, 2010.

[34] Y. Xiong, W. Wang, Y. Shi et al., "Investigation on surface roughness, residual stress and fatigue property of milling in-situ TiB2/7050Al metal matrix composites," *Chinese Journal of Aeronautics*, vol. 34, no. 4, pp. 451–464, 2021.

[35] X. Liu, W. Wang, R. Jiang et al., "Analytical model of cutting force in axial ultrasonic vibration-assisted milling in-situ TiB2/7050Al PRMMCs," *Chinese Journal of Aeronautics*, vol. 34, no. 4, pp. 160–173, 2021.

[36] M. El-Gallab and M. Sklad, "Machining of Al/SiC particulate metal matrix composites Part II: workpiece surface integrity," *Journal of Materials Processing Technology*, vol. 83, no. 1–3, pp. 277–285, 1998.

[37] N. Muthukrishnan, M. Murugan, and K. Prahlada Rao, "Machinability issues in turning of Al-SiC (10p) metal matrix composites," *International Journal of Advanced Manufacturing Technology*, vol. 39, no. 3–4, pp. 211–218, 2008.

[38] S. S. Joshi, N. Ramakrishnan, and P. Ramakrishnan, "Analysis of chip breaking during orthogonal machining of Al/SiCp composites," *Journal of Materials Processing Technology*, vol. 88, no. 1-3, pp. 90–96, 1999.